Title 論文題目	Six-transmembrane epithelial antigen of the prostate 1 accelerates cell proliferation by targeting c-Myc in liver cancer cells (STEAP1はc-Mycを介し肝細胞癌細胞の増殖を亢進させる)
Author(s) 著者	飯島, 一飛
Degree number 学位記番号	甲第3151号
Degree name 学位の種別	博士(医学)
Issue Date 学位取得年月日	2022-03-31
Original Article 原著論文	Oncol Lett. 2021 Jul;22(1):546
Doc URL	
DOI	10.3892/ol.2021.12807
Resource Version	Author Edition

Six-transmembrane epithelial antigen of the prostate 1 accelerates cell proliferation by targeting c-Myc in liver cancer cells

KAZUTAKA IIJIMA[1*], HAJIME NAKAMURA[1*], KOHICHI TAKADA[1], NAOTAKA HAYASAKA[1], TOMOHIRO KUBO[1], YUI UMEYAMA[1], SATOSHI IYAMA[2], KOJI MIYANISHI[1], MASAYOSHI KOBUNE[2] and JUNJI KATO[1]

Departments of [1]Medical Oncology and [2]Hematology, Sapporo Medical University School of Medicine, Sapporo, Hokkaido 060-8543, Japan

Received March 5, 2021; Accepted May 11, 2021

DOI: 10.3892/ol.2021.12807

Abstract. Six-transmembrane epithelial antigen of the prostate 1 (STEAP1) has emerged as an ideal target in cancer therapeutics. However, the functions of STEAP1 in liver cancer remain unexplored. The current study aimed to characterize the biological roles of STEAP1 in liver cancer. *STEAP1* expression was upregulated in tumor tissues, and high *STEAP1* expression was associated with poor clinical outcomes in patients with liver cancer, according to several publicly available datasets. *STEAP1* silencing using small interfering RNA inhibited cell proliferation and was accompanied by G_1 arrest induced by the suppression of cyclin D1 and the promotion of p27. *STEAP1* silencing suppressed c-Myc expression, which was identified as a component in STEAP1 signal transduction by mining publicly available datasets and was then confirmed by PCR array. In conclusion, the knockdown of *STEAP1* in liver cancer cell lines led to inhibition of cell proliferation involving G_1 arrest by suppressing c-Myc. The present study provides a preclinical concept for *STEAP1* as a druggable target in liver cancer.

Introduction

Primary liver cancer is estimated to be the third leading cause of cancer-related deaths worldwide, accounting for 830,000 deaths each year (1). Hepatocellular carcinoma (HCC) is the most common type of primary liver cancer comprising 75-85% of cases (1). Despite recent advances in multikinase inhibitors, such as sorafenib, regorafenib, and lenvatinib, as well as anti-vascular endothelial growth factor therapies and immune check point inhibitors, advanced HCC has a dismal prognosis (2-5). An exploration of the molecular characteristics of liver cancer is needed to develop more effective therapeutics.

A well characterized oncoprotein, c-Myc contributes to the pathogenesis of a broad range of human cancers, including liver cancer (6). Overexpression of c-Myc is associated with a poor prognosis (7). The amplification of *c-Myc* and alterations of proximal c-Myc network members have been identified in over 30% and 70% of HCC cases, respectively (8). Such findings highlight c-Myc as an attractive target for liver cancer therapeutics. However, its structure, which lacks a druggable hydrophobic pocket, and its nuclear localization have hampered the development of specific inhibitors of c-Myc (9). Certainly, ongoing clinical trials of c-Myc inhibitors are non-existent, except for a trial involving 90-amino acid peptide as a dominant negative inhibitor (10). Specifically, it is critical to seek druggable targets in the c-Myc pathway to combat c-Myc-driven liver cancer.

Six-transmembrane epithelial antigen of the prostate 1 (STEAP1), which was initially identified in prostate cancer cells and is expressed at low levels in normal cells, is a cell surface protein (11) that is over-expressed in many human cancers (12). STEAP1 has thus emerged as an ideal target in cancer therapeutics. STEAP1 is believed to play a physiological role as an ion channel and transporter (13). Additionally, structural analyses using a cryo-electron microscopy revealed that STEAP1 works as a ferric reductase when binding to the NADPH-binding domain of STEAP4 (14). In contrast, the pathological functions of STEAP1 in cancer cells have been largely unexplored. We recently discovered that high expression of STEAP1 lead to the suppression of reactive oxygen species (ROS) that escaped from apoptosis via a NF-E2-related factor 2 (NRF2) pathway in colorectal cancer cells (15). However, the roles of STEAP1 in liver cancer pathogenesis remain completely unknown.

Here, we sought to characterize the biological roles of STEAP1 in liver cancer. We identified that *STEAP1* transcript levels were significantly increased in liver cancer compared to normal liver cells, and that such high levels were associ-

Correspondence to: Dr Kohichi Takada, Department of Medical Oncology, Sapporo Medical University School of Medicine, South-1, West-16, Chuo, Sapporo, Hokkaido 060-8543, Japan
E-mail: author@mail.com

*Contributed equally

Key words: six-transmembrane epithelial antigen of the prostate 1, c-Myc, G1 arrest, liver cancer, hepatocellular carcinoma, cancer therapeutics

ated with a poor prognosis. The knockdown of *STEAP1* led to cell-growth inhibition accompanied by G_1 arrest by targeting the suppression of c-Myc, which was discovered by mining publicly available databases. Our findings yield a new treatment strategy targeting the STEAP1-c-Myc axis in liver cancer.

Materials and methods

Databases and gene expression data analysis. Gene expression levels of *STEAP1* in non-tumor and liver cancer tissues were evaluated using gene expression profiles of GSE14520 and GSE36376 from the Gene Expression Omnibus, a public and freely available database. The GSE14520 dataset includes 488 samples of 241 non-cancerous and 247 cancerous hepatic tissues. These datasets have been widely used and well accepted in bioinformatics analysis of liver cancer. The GSE36376 dataset includes 433 samples consisting of 193 non-cancerous hepatic tissues and 240 cancerous tissues. The correlation between *STEAP1* levels and clinical outcomes of patients with liver cancer was investigated using GSE14520 and the Cancer Genome Atlas Program (TCGA) (16). We used a receiver operating characteristic curve to determine the cutoff value. In total, 247 patients from the GSE14520 dataset and 360 patients from TCGA, all with liver cancer, were divided into two groups having high or low levels of *STEAP1*, respectively. Kaplan-Meier analyses of survival were performed based on these groups. Statistical analyses were performed using EZR software version 1.33 (17).

Gene set enrichment analysis (GSEA) was performed using the open source software, GSEA 4.0.3. Initially, we set two groups (*STEAP1*_high and *STEAP1*_low) in GSE14520-GPL3921, which includes 225 liver cancer samples in total. We conducted GSEA of the two groups using Hallmark gene sets. Gene sets showing a NOM P-val. (P-value) <0.05 and false discovery rate (FDR) Q-val. (FDR) <0.25 were considered significant. Differentially expressed genes (DEGs) between these two groups were identified using an online tool, GEO2R, with |logFC| >1.5 and an adjusted P-value <0.05.

Cell lines and culture conditions. HepG2 and Hep3B cell lines were purchased from the American Type Culture Collection; these were authenticated by short tandem repeat DNA profiling prior to all experiments. Both cell lines were cultured in DMEM containing 10% fetal bovine serum (FBS), 2 μM L-glutamine and 1% penicillin-streptomycin (the medium and all supplements from Sigma-Aldrich; Merck KGaA).

Inhibition of STEAP1 expression by small-interfering RNA. Control small-interfering RNA (siRNA; Control; #4390843; Thermo Fisher Scientific, Inc.) and two independent siRNAs targeting human *STEAP1* (siSTEAP1; D-003713-01: 5'-GGA GAGAAUUUCACUAUAU-3' and D-003713-02: 5'-UAAAGA AGAUGCCUGGAUU-3'; Dharmacon) were transfected using Lipofectamine RNAiMAX (Thermo Fisher Scientific, Inc.) according to the manufacturer's protocol. Cells were seeded at a density of $3x10^5$ cells/well into 6-well plates and cultured for 24 h at 37˚C. Subsequently, cells were transfected with control siRNA or siRNA targeting human *STEAP1*, and incubated for 72 h at 37˚C. Final siRNA used per well was 25 pmol. After incubation, floating cells in media were collected, adhesive cells were washed and collected, and both were immediately used for experiments.

Reverse transcription-quantitative PCR (RT-qPCR). Total RNA was extracted using TRIzol Reagent (Thermo Fisher Scientific) according to the manufacturer's protocol. Subsequently, complementary (c)DNA was synthesized from the RNA using a SuperScript VILO cDNA synthesis kit (Thermo Fisher Scientific). qPCR was performed with an Applied Biosystems 7300 Real-time PCR system (Applied Biosystems; Thermo Fisher Scientific, Inc.). The analysis of target genes (*STEAP1* and *c-Myc*) was conducted in quadruplicate using a POWER SYBR-Green Master Mix (Thermo Fisher Scientific, Inc.) as previously described (18). The thermal profile of the qPCR program consisted of 2 min at 50˚C, 10 min at 95˚C, 40 cycles of 15 sec at 95˚C and 1 min at 60˚C, and a dissociation stage at the end of the run from 60˚C to 95˚C. Transcript levels were normalized to β-actin expression and analyzed using the $2^{-\Delta\Delta Cq}$ method. The following PCR primers were designed: 5'-CCCTTCTACTGGGCACAATACA-3' and 5'-GCATGG CAGGAATAGTATGCTTT-3' for *STEAP1*; 5'-TTTTTCGGG TAGTGGAAAACC-3' and 5'-GCAGTAGAAATACGGCTG CAC-3' for *c-Myc*; and 5'-GGCATCCTCACCCTGAAGTA-3' and 5'-GAAGGTGTGGTGCCAGATTT-3' for *β-actin*.

Western blotting. As previously described (19), cells were solubilized in radioimmunoprecipitation assay lysis buffer (50 mM Tris-HCl, pH 7.5, 1% NP-40, 0.5% Na-deoxycholate, 1 mM EDTA, 150 mM NaCl, 1 mM EGTA, and protease inhibitor cocktail; Sigma-Aldrich; Merck KGaA), and centrifuged at 12,000 x g for 10 min. The supernatants were collected, and protein concentrations were determined using a bicinchoninic acid Protein Assay Kit (Thermo Fisher Scientific, Inc.). Equal amounts of protein were separated on MULTIGEL II mini gels (Cosmo Bio Co., Ltd.) and transferred to polyvinylidene fluoride membranes using a QBlot Kit (ATTO, Tokyo, Japan). The blots were probed using the following primary antibodies: anti-*STEAP1* (sc25514; Santa Cruz Biotechnology), anti-*STEAP1* (#88677; Cell Signaling Technology), anti-cyclin D1 (#2987; Cell Signaling Technology,), anti-p27 Kip1 (#3686; Cell Signaling Technology), anti-c-Myc (OP10L; EMD Biosciences), and anti-actin-horse radish peroxidase (HRP; sc-47778; Santa Cruz Biotechnology).

Evaluation of cell proliferation. Hepatocellular carcinoma cells were seeded at a density of $2x10^3$ cells/well into 96-well plates. Control siRNA or two independent siRNAs targeting human *STEAP1* were transfected 24 h after seeding. Cell viability was assessed at 0, 24, 48 and 72 h using a WST-1 assay (Premix WST-a Cell Proliferation Assay; Takara Bio) and Infinite M1000 Pro microplate reader (Tecan Japan). A growth curve was constructed by plotting absorbance against time.

Cell cycle analysis. Liver cancer cells were seeded at a density of $3x10^5$ cells/well into 6-well plates and cultured for 24 h. Subsequently, cells were transfected with control siRNA or an siRNA targeting human *STEAP1*, and incubated for 72 h. After incubation, floating cells in media were collected and adhesive

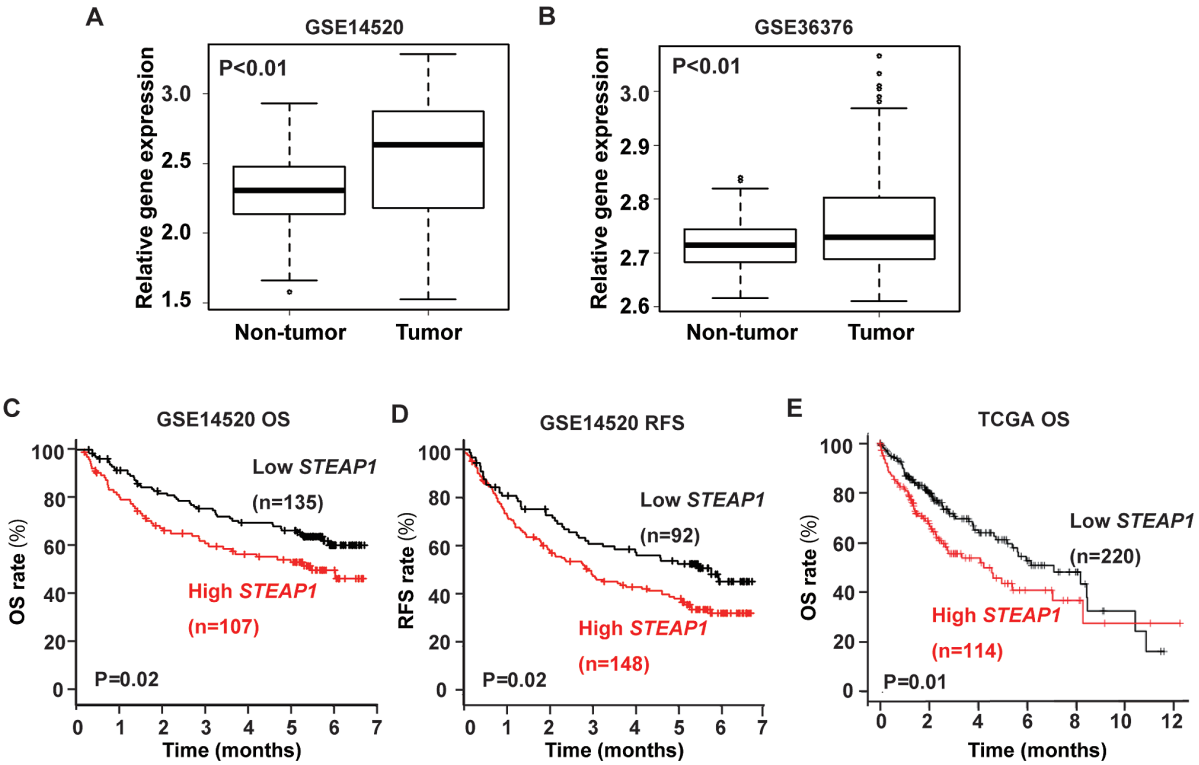

Figure 1. *STEAP1* expression is upregulated and associated with poor survival in patients with liver cancer. Publicly accessible gene expression profiling datasets, (A) GSE14520 and (B) GSE36376, were obtained from the Gene Expression Omnibus and analyzed to evaluate *STEAP1* expression in patients with liver cancer. Associations between *STEAP1* expression and (C) OS and (D) RFS in GSE14520, and (E) OS in TCGA were evaluated using the Kaplan-Meier method. STEAP1, six-transmembrane epithelial antigen of the prostate 1; OS, overall survival; RFS, recurrence-free survival; TCGA, The Cancer Genome Atlas.

cells were washed, fixed in ethanol, and stained with propidium iodide using a cell-cycle analysis kit (FxCycle PI/RNase Staining Solution; Thermo Fisher Scientific), followed by analysis on a BD FACS II (BD Biosciences) instrument using FACSDiva (BD Biosciences) as previously described (20).

Apoptosis assay. Apoptosis was evaluated using an Annexin V/7-amino-actinomycin (AAD) staining kit (BD Biosciences). Liver cancer cells were seeded at a density of $3x10^5$ cells/well into 6-well plates and cultured for 24 h. Subsequently, cells were transfected with control siRNA or an siRNA targeting human *STEAP1*, and incubated for 72 h. After incubation, floating cells in media were collected and adhesive cells were washed, stained with Annexin V and 7-AAD, and analyzed on a BD FACSCanto II (BD Biosciences) instrument using FACSDiva (BD Biosciences) as previously described (21).

PCR array. Total RNA was reverse-transcribed using an RT^2 First Strand Kit (Qiagen). PCR array was performed using RT^2 Profiler™ PCR Array Human MYC Targets (PAHS-177Z; Qiagen) according to the manufacturer's protocol.

Statistical analysis. The significance of differences was determined by Student's t-test, Mann-Whitney U test, log-rank test or one-way ANOVA followed by Bonferroni's post-hoc test, as appropriate. Pearson's correlation was used to perform the correlation analysis. All statistical analyses were performed using EZR software version 1.33 (17). Statistical significance was defined as $P<0.05$.

Results

STEAP1 is up-regulated and significantly associated with poor overall survival and recurrence-free survival in liver cancer. We first investigated the expression of *STEAP1* in patients with liver cancer using publicly accessible datasets (GSE14250 and GSE36376) from the Gene Expression Omnibus. In both datasets, *STEAP1* is over-expressed in liver cancer tissues compared to non-cancerous hepatic tissues (Fig. 1A and B). Next, we evaluated the correlation between *STEAP1* expression and survival in patients with liver cancer using GSE14520 and TCGA datasets. Patients with high *STEAP1* expression presented with significantly shorter overall survival (OS) and recurrence-free survival (RFS) in GSE14520 and significantly shorter OS in TCGA (Fig. 1C-E). These data imply that STEAP1 may have oncogenic functions in liver cancer.

Knockdown of STEAP1 inhibits proliferation of liver cancer cell lines. To evaluate the effect of STEAP1 on liver cancer, we performed *STEAP1* silencing using an RNA interference method in two different liver cancer cell lines, HepG2 and Hep3B. Knockdown efficiency was examined by RT-qPCR and western blot. STEAP1 expression in these cell lines was significantly down-regulated 72 h after transfection of two independent siRNAs (Fig. 2A, B, D and E). We next evaluated the impact of *STEAP1* silencing on liver cancer cell lines using WST-1 assays. *STEAP1* silencing significantly reduced proliferation in both cell lines (Fig. 2C and F). Based on these data, we concluded that STEAP1 activated proliferation in liver cancer cell lines.

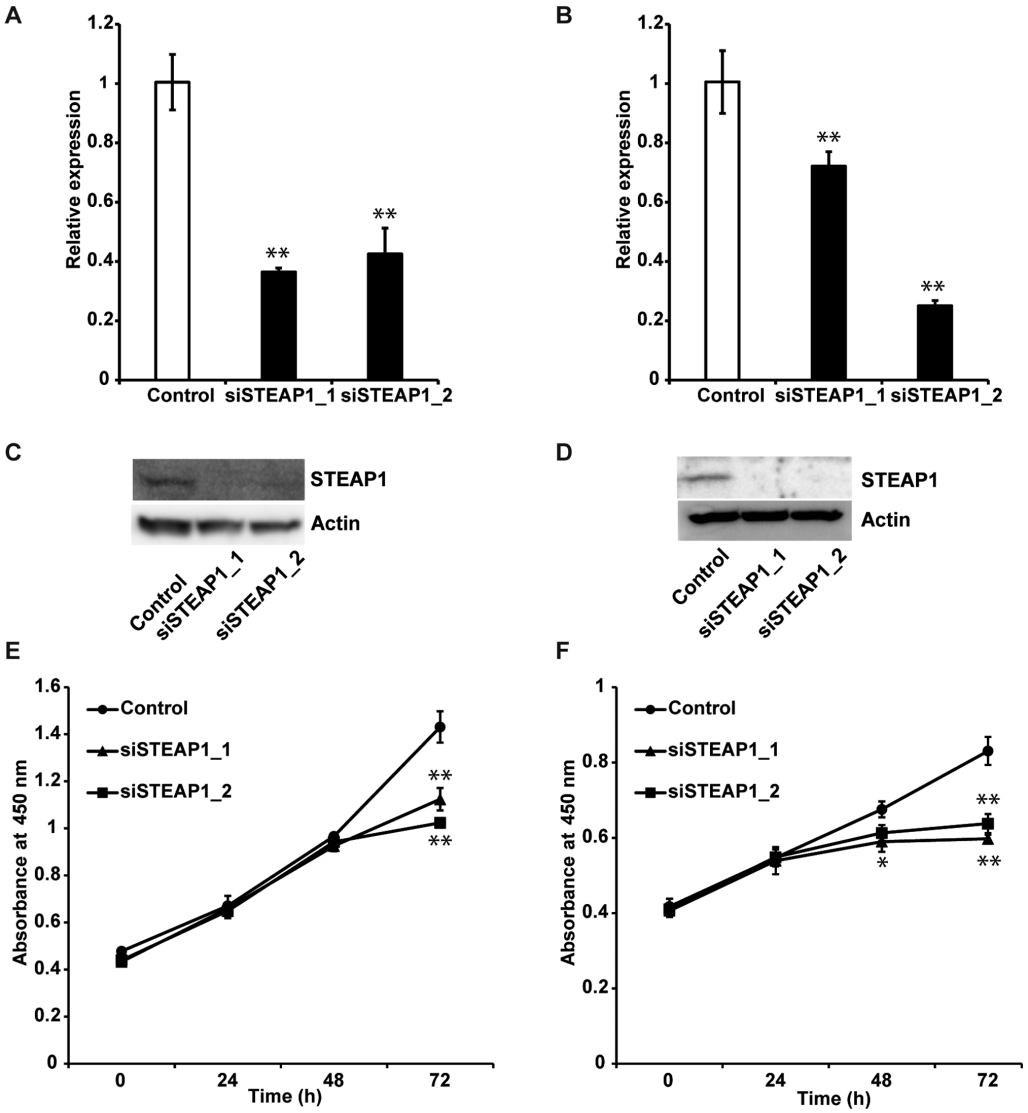

Figure 2. Knockdown of *STEAP1* leads to inhibition of cell proliferation in different liver cancer cell lines. Two different liver cancer cell lines, HepG2 and Hep3B, were transfected with non-targeting control siRNA and two independent siRNAs targeting (siSTEAP1_1 and siSTEAP1_2). Efficiency of knockdown was evaluated using RT-qPCR and western blotting. RT-qPCR in (A) HepG2 and (B) Hep3B cells. Western blotting in (C) HepG2 and (D) Hep3B. Data of RT-qPCR experiments are shown as the mean of quadruplicate measurements ± SD. Cell proliferation of two different liver cancer cell lines, (E) HepG2 and (F) Hep3B, was evaluated using a WST-1 assay at 0, 24, 48 and 96 h after siRNA transfection. Data are presented as the mean of triplicate measurements ± SD. *P<0.05 and **P<0.01 vs. control. RT-qPCR, reverse transcription-quantitative PCR; siRNA, small interfering RNA; STEAP1, six-transmembrane epithelial antigen of the prostate 1.

STEAP1 silencing promotes G_1 arrest in liver cancer cell lines. To evaluate the mechanism of decreasing proliferation in response to the knockdown of *STEAP1*, we examined the effects of *STEAP1* silencing on the cell cycle in the liver cancer cell lines, HepG2 and Hep3B. *STEAP1* silencing significantly induced G_1 arrest in both liver cancer cell lines (Fig. 3A and B). We also performed a flow cytometry analysis using Annexin V/7AAD staining to evaluate the rate of apoptosis. However, an increased percentage of apoptosis was not observed in *STEAP1*-silenced liver cancer cell lines (Fig. S1A and B). To analyze the mechanism of G_1 arrest in HCC cell lines induced by the knockdown of *STEAP1*, we evaluated protein levels of several cell-cycle-related proteins in liver cancer cell lines using western blot. The expression of the G_1 arrest-associated protein, cyclin D1, was decreased, whereas the expression of p27, which promotes cell-cycle arrest, was apparently increased (Fig. 3C).

c-Myc target genes were significantly enriched in patients with liver cancer showing high STEAP1 expression. To clarify the pathways related to STEAP1, we first extracted DEGs between low and high *STEAP1* liver cancer samples in a publicly accessible dataset, GSE14520-GPL3921, using GEO2R. The significant DEGs with |logFC| >1.5 and adjusted P-value < 0.05 are highlighted in red and blue colors. Each gene was represented as a volcano plot (Fig. 4A) and listed in a table (Table I). Next, we conducted GSEA to explore the gene sets regulated by STEAP1 in liver cancer and found five pathways which were significantly enriched (NOM P-val <0.05 and FDR Q-val <0.25; Fig. 4B, Fig. S2, and Table SI). The genes belonging to MYC_TARGET_V2 were the most significantly enriched among these five pathways (Fig. 4C and D). Based on these findings, we hypothesized the existence of a relationship between STEAP1 and c-Myc in liver cancer. To confirm this, we evaluated their expression using the publicly accessible data-

Table I. List of significant DEGs in samples with high and low *STEAP1* expression in publicly accessible gene expression profiling dataset, GSE14520-GPL3921.

A, Upregulated DEGs

Symbol	Gene name	log_2 ratio	Adjusted P-value
AFP	α fetoprotein	2.28	0.0197
SULT1C2	Sulfotransferase family 1C member 2	2.23	0.0000113
MT1E	Metallothionein 1E	2.09	0.0000135
ABCB1	ATP binding cassette subfamily B member 1	1.99	0.0000268
MT1G	Metallothionein 1G	1.96	0.0000135
GPX2	Glutathione peroxidase 2	1.92	0.00308
C9	Complement component 9	1.92	0.00971
MT1H	Metallothionein 1H	1.91	0.0000105
SPP1	Secreted phosphoprotein 1	1.91	0.0104
MT1X	Metallothionein 1X	1.86	0.0000241
REG3A	Regenerating family member 3α	1.83	0.0215
ROBO1	Roundabout guidance receptor 1	1.82	0.0000441
LCN2	Lipocalin 2	1.8	0.00455
MYC	v-myc avian myelocytomatosis viral oncogene homolog	1.74	0.00023
MT1M	Metallothionein 1M	1.71	0.000015
TSPAN8	Tetraspanin 8	1.67	0.00928
PLPPR1	Phospholipid phosphatase related 1	1.64	0.00000564
MT1X	Metallothionein 1X	1.64	0.000126
MT1F	Metallothionein 1F	1.63	0.0000604
BCHE	Butyrylcholinesterase	1.61	0.0103
MT1HL1	Metallothionein 1H-like 1	1.6	0.0000192
MTTP	Microsomal triglyceride transfer protein	1.6	0.000745
SQSTM1	Sequestosome 1	1.59	0.000114
RELN	Reelin	1.59	0.0144
CXCL5	C-X-C motif chemokine ligand 5	1.57	0.000184
TRIM16L///TRIM16	Tripartite motif containing 16-like///tripartite motif containing 16	1.57	0.000923
AKR1C4	Aldo-keto reductase family 1, member C4	1.57	0.00464
CCL20	C-C motif chemokine ligand 20	1.56	0.00949
COL2A1	Collagen type II α 1 chain	1.55	0.0134
YBX3	Y-box binding protein 3	1.54	0.0000268
IGF2BP3	Insulin like growth factor 2 mRNA binding protein 3	1.54	0.00289

B, Downregulated DEGs

Symbol	Gene name	log_2 ratio	Adjusted P-value
SLPI	Secretory leukocyte peptidase inhibitor	-3.17	$3.31x10^{-08}$
GNMT	Glycine N-methyltransferase	-1.88	0.0016
SPP2	Secreted phosphoprotein 2	-1.82	0.00581
LGALS4	Galectin 4	-1.79	0.0169
CYP7A1	Cytochrome P450 family 7 subfamily A member 1	-1.55	0.0472
SLC22A1	Solute carrier family 22 member 1	-1.55	0.03
PPP1R1A	Protein phosphatase 1 regulatory inhibitor subunit 1A	-1.53	0.00516
CHI3L1	Chitinase 3 like 1	-1.52	0.12

DEGs, differentially expressed genes; STEAP1, six-transmembrane epithelial antigen of the prostate 1.

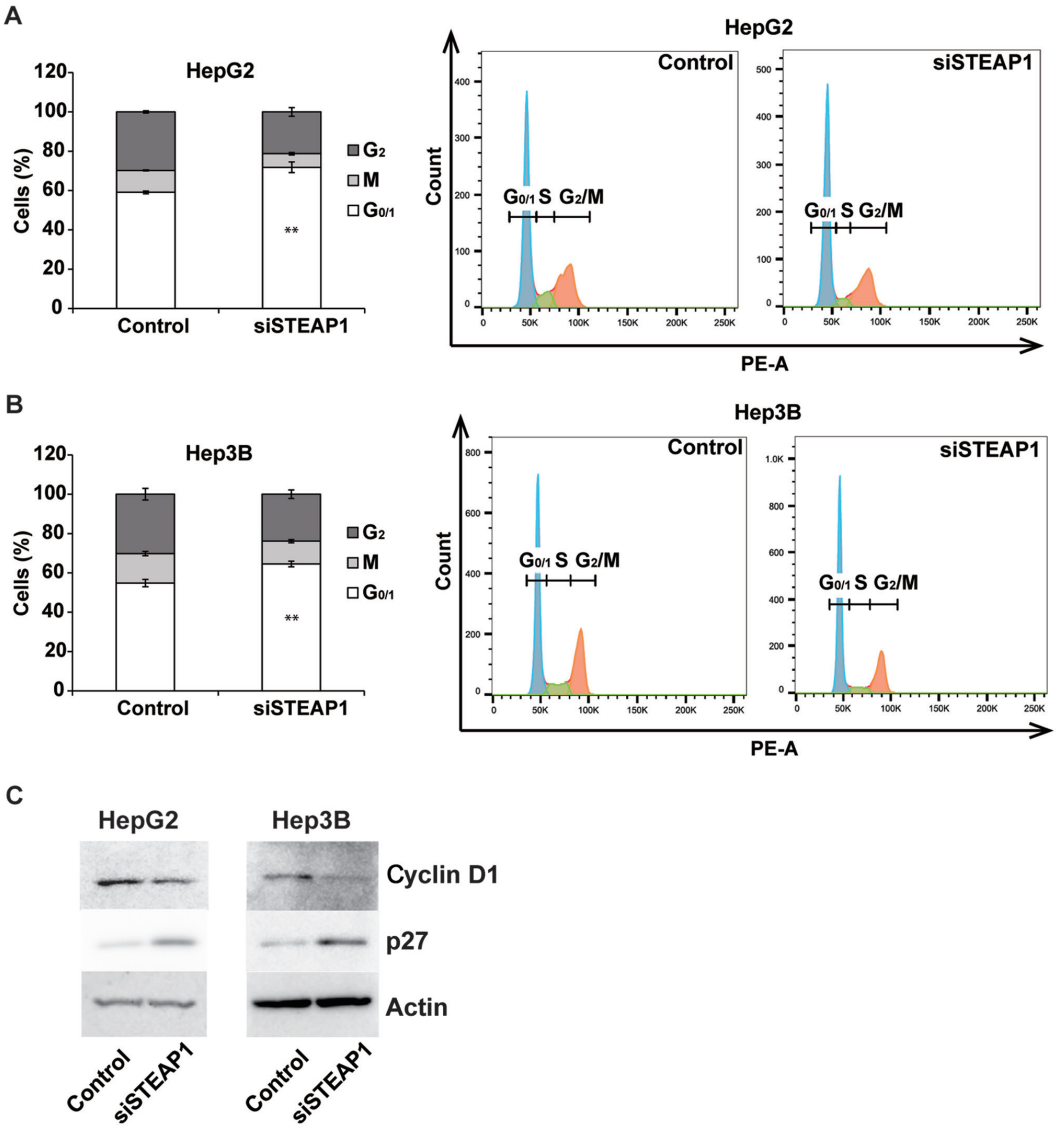

Figure 3. *STEAP1* silencing triggers G_1 arrest in liver cancer cell lines. Two different liver cancer cell lines, (A) HepG2 and (B) Hep3B, were transfected with non-targeting control siRNA or siSTEAP1. Cells were stained with propidium iodide 72 h after siRNA transfection. Subsequently, cell cycles were analyzed by flow cytometry. The percentage of $G_{0/1}$ cells transfected with siSTEAP1 was compared to that of cells transfected with non-targeting control siRNA. Data are presented as the mean of triplicate measurements ± SD. **P<0.01. (C) Two different liver cancer cell lines, HepG2 and Hep3B, were transfected with non-targeting control siRNA or siSTEAP1. Cell cycle-associated proteins were analyzed by western blotting. siRNA, small interfering RNA; STEAP1, six-transmembrane epithelial antigen of the prostate 1.

sets, GSE14250, GSE36376, and TCGA. Pearson's correlation coefficient analysis revealed a significant positive relationship between *STEAP1* and *c-Myc* in all datasets (Fig. 4E-G).

STEAP1 regulates c-Myc and its related genes in liver cancer cell lines. To confirm the relationship between STEAP1 and c-Myc in liver cancer, we evaluated the expression of c-Myc after *STEAP1* knockdown in HepG2 and Hep3B cell lines by RT-qPCR and western blot. As we expected, downregulation of c-Myc was observed in both cell lines when transfected with siRNA targeting *STEAP1* compared to non-targeting siRNA (Fig. 5A-D). Next, we conducted a PCR array to analyze components of c-Myc-related genes; most were significantly downregulated by *STEAP1* silencing (Figs. 5E and S3). Taken together, our data suggest that c-Myc lies downstream of STEAP1, and that the STEAP1-c-Myc pathway promotes cell proliferation and cell-cycle progression in liver cancer.

Discussion

Recently, treatment options for HCC have been expanding as new drugs are approved (2-5). However, unresectable HCC is an incurable disease; its median overall survival remains around a year (22). Thus, the further exploration of novel molecularly-based therapies is required to improve survival in patients with advanced HCC. c-Myc is a high priority target of liver cancer therapeutics because its pathological functions exist in a subset of liver cancer cases. The structure of c-Myc has hampered the development of c-Myc-specific inhibitors and highlights the need for further investigations of novel c-Myc signaling components as potential targets for liver cancer therapeutics. The current study elucidated STEAP1 as a member of the c-Myc signal transduction pathway using *in vitro* and bioinformatic analyses. Inhibition of *STEAP1* led to the suppression of cell growth accompanied by G_1 arrest in liver cancer, encour-

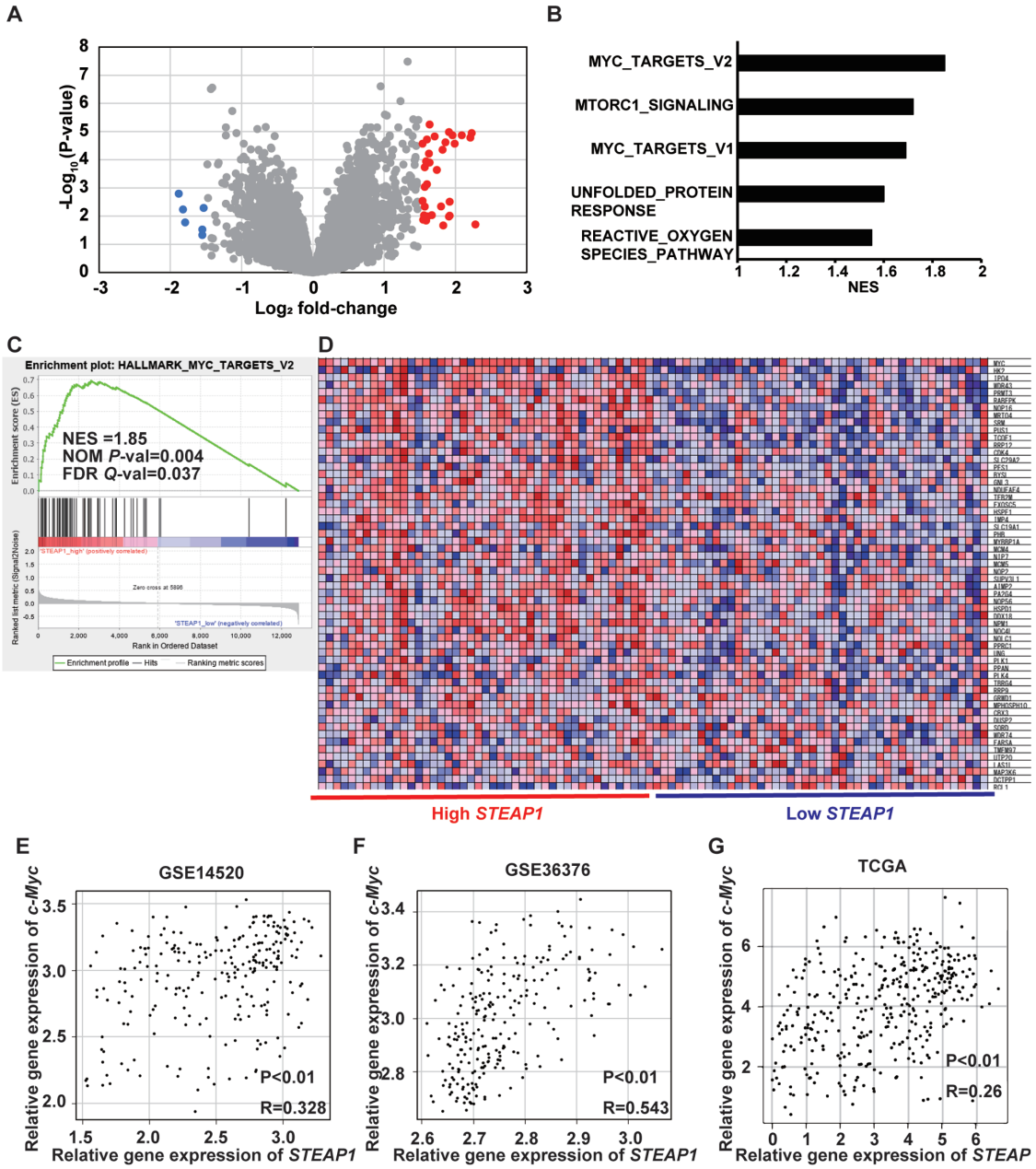

Figure 4. *c-Myc* target genes are significantly enriched in patients with liver cancer with high *STEAP1* expression. (A) Volcano plot of DEGs in samples with high and low *STEAP1* expression in a publicly accessible gene expression profiling dataset, GSE14520-GPL3921. Significant DEGs were defined as P<0.05 and a |log fold-change| >1.5. Red indicates upregulated genes, blue indicates downregulated genes and gray indicates non-DEGs. (B) Gene Set Enrichment Analysis was performed to explore the gene sets regulated by *STEAP1* in liver cancer. Bar graph showing significantly enriched Hallmark gene sets in patients with liver cancer with high *STEAP1* expression. (C) Enrichment plot presentation of MYC_TARGETS_V2. (D) Heat map presentation of genes included in MYC_TARGET_V2 between samples with high and low *STEAP1* expression. Correlation between *STEAP1* and *c-Myc* in samples with liver cancer using publicly accessible gene expression profiling datasets: (E) GSE14520, (F) GSE36376 and (G) TCGA. DEGs, differentially expressed genes; NES, normalized enrichment score; NOM P-val, nominal P-value; FDR Q-val, false discovery rate Q-value; STEAP1, six-transmembrane epithelial antigen of the prostate 1.

aging the development of STEAP1 inhibitors as therapeutics for STEAP1-c-Myc axis-driven liver cancer. Additionally, STEAP1 is an attractive target for antibody drug conjugates (ADC) in cancers because it is expressed on the plasma membrane (11). In fact, DSTP3086S, an ADC-targeting STEAP1, has been introduced for patients with metastatic castration-resistant prostate cancer; it has been evaluated as safe and shows promising therapeutics (23). Therefore, an ADC-targeting STEAP1 can be used for patients with liver cancer, who, according to our data, show the overexpression of STEAP1 in cancerous hepatic tissue compared to adjacent non-cancerous parts (Fig. 1A and B).

In our previous work, we demonstrated that *STEAP1* knockdown led to apoptosis in colorectal cancer cells in an NRF2-dependent fashion, corresponding to the increased production of ROS (15). As shown in Fig. S4, intracellular ROS levels were increased by *STEAP1* inhibition as found in our previous work (Fig. S4A and B). Furthermore, GSEA revealed an ROS-related pathway was significantly enriched in patients with liver cancer showing upregulated *STEAP1* (Fig. S2D). However, as mentioned above, apoptotic cells were not increased by *STEAP1* inhibition in liver cancer cells (Fig. S1A and B). In addition, we found no statistical correlation between *STEAP1*

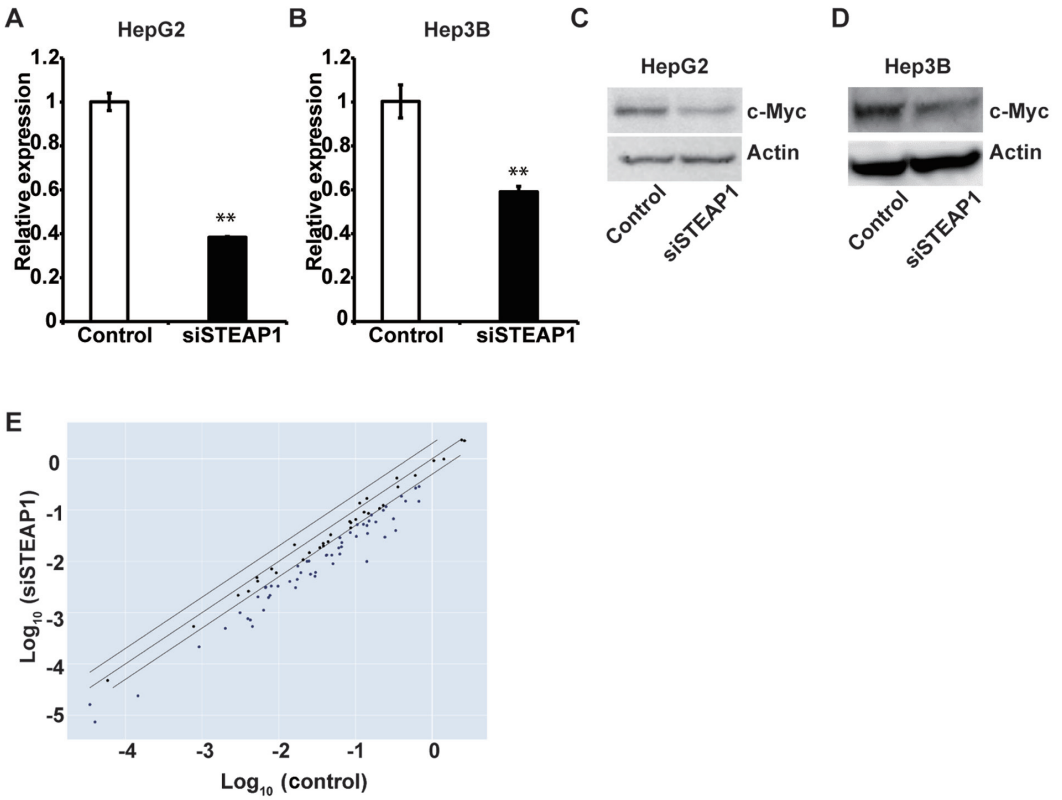

Figure 5. Inhibition of *STEAP1* suppresses c-Myc and its downstream target genes in liver cancer cell lines. Two different liver cancer cell lines (HepG2 and Hep3B) were transfected with non-targeting control siRNA and si*STEAP1*. c-Myc expression was evaluated by RT-qPCR and western blotting. RT-qPCR in (A) HepG2 and (B) Hep3B cells. Western blotting in (C) HepG2 and (D) Hep3B cells. Data of RT-qPCR experiments are shown as the mean of quadruplicate measurements ± SD. **P<0.01 vs. control. (E) Scatterplot representation of the *c-Myc* targeted genes validated by PCR array in HepG2 cells. siRNA, small interfering RNA; *STEAP1*, six-transmembrane epithelial antigen of the prostate 1; RT-qPCR, reverse transcription-quantitative PCR.

and *NRF2* in three individual datasets (GSE14520, GSE36376 and TCGA; Fig. S4C-E). Furthermore, previous studies reported that c-Myc generates ROS in liver cancer cells (24,25). However, the current study demonstrated that STEAP1 leads the increased expression of c-Myc and reduced ROS production in liver cancer cells. These results seem inconsistent, suggesting the existence of an NRF2 or c-Myc independent ROS-related pathway in the regulation of STEAP1-mediated cell growth. Additionally, others have shown *STEAP1* silencing induced cell growth inhibition, which was associated with decreased levels of ROS in cases of Ewing sarcoma (26). These results suggest the existence of multiple pathways between STEAP1 and ROS in a cancer-type specific manner. Accordingly, our next steps include exploring the relationship between STEAP1 and ROS in STEAP1-driven cancer cells.

In summary, this study provides a preclinical concept for STEAP1 as a druggable target in liver cancer, an often fatal cancer. The STEAP1-c-Myc axis has potential as an attractive and promising therapeutic target in liver cancer, and its manipulation will lead to the development of a novel strategy to conquer this malignant disease.

Acknowledgements

The authors would like to thank Ms. Kei Yoneguchi (Department of Medical Oncology, Sapporo Medical University School of Medicine, Sapporo, Hokkaido, Japan) for her technical assistance.

Funding

The present study was funded by a grant from Japan Society for the Promotion of Science (grant no. 19K08397)

Availability of data and materials

The datasets generated and/or analyzed during the current study are available in the Gene Expression Omnibus repository, https://www.ncbi.nlm.nih.gov/geo/query/acc.cgi?acc=GSE173813.

Authors' contributions

KT, HN and KI were responsible for the conception and design of the study and for confirming the authenticity of the data. NH, TK, YU, SI, KM, MK and JK performed the analysis and interpretation of data. HN and KT drafted the manuscript. JK critically reviewed and revised the manuscript. All authors read and approved the final manuscript.

Ethics approval and consent to participate

Not applicable.

Patient consent for publication

Not applicable.

Competing interests

The authors declare that they have no competing interests.

References

1. Sung H, Ferlay J, Siegel RL, Laversanne M, Soerjomataram I, Jemal A and Bray F: Global cancer statistics 2020: GLOBOCAN estimates of incidence and mortality worldwide for 36 cancers in 185 countries. CA Cancer J Clin 71: 209-249.
2. Llovet JM, Ricci S, Mazzaferro V, Hilgard P, Gane E, Blanc JF, de Oliveira AC, Santoro A, Raoul JL, Forner A, *et al*; SHARP Investigators Study Group: Sorafenib in advanced hepatocellular carcinoma. N Engl J Med 359: 378-390, 2008.
3. Bruix J, Qin S, Merle P, Granito A, Huang YH, Bodoky G, Pracht M, Yokosuka O, Rosmorduc O, Breder V, *et al*; RESORCE Investigators: Regorafenib for patients with hepatocellular carcinoma who progressed on sorafenib treatment (RESORCE): A randomised, double-blind, placebo-controlled, phase 3 trial. Lancet 389: 56-66, 2017.
4. Kudo M, Finn RS, Qin S, Han KH, Ikeda K, Piscaglia F, Baron A, Park JW, Han G, Jassem J, *et al*: Lenvatinib versus sorafenib in first-line treatment of patients with unresectable hepatocellular carcinoma: A randomised phase 3 non-inferiority trial. Lancet 391: 1163-1173, 2018.
5. Finn RS, Qin S, Ikeda M, Galle PR, Ducreux M, Kim TY, Kudo M, Breder V, Merle P, Kaseb AO, *et al*; IMbrave150 investigators: Atezolizumab plus bevacizumab in unresectable hepatocellular carcinoma. N Engl J Med 382: 1894-1905, 2020.
6. Stine ZE, Walton ZE, Altman BJ, Hsieh AL and Dang CV: MYC, metabolism, and cancer. Cancer Discov 5: 1024-1039, 2015.
7. Abou-Elella A, Gramlich T, Fritsch C and Gansler T: c-myc amplification in hepatocellular carcinoma predicts unfavorable prognosis. Mod Pathol 9: 95-98, 1996.
8. Schaub FX, Dhankani V, Berger AC, Trivedi M, Richardson AB, Shaw R, Zhao W, Zhang X, Ventura A, Liu Y, *et al*; Cancer Genome Atlas Network: Pan-cancer alterations of the MYC oncogene and its proximal network across the Cancer Genome Atlas. Cell Syst 6: 282-300.e2, 2018.
9. Duffy MJ and Crown J: Drugging 'undruggable' genes for cancer treatment: Are we making progress? Int J Cancer 148: 8-17, 2021.
10. Massó-Vallés D and Soucek L: Blocking Myc to treat cancer: Reflecting on two decades of omomyc. Cells 9: 883, 2020.
11. Hubert RS, Vivanco I, Chen E, Rastegar S, Leong K, Mitchell SC, Madraswala R, Zhou Y, Kuo J, Raitano AB, *et al*: STEAP: A prostate-specific cell-surface antigen highly expressed in human prostate tumors. Proc Natl Acad Sci USA 96: 14523-14528, 1999.
12. Moreaux J, Kassambara A, Hose D and Klein B: STEAP1 is overexpressed in cancers: A promising therapeutic target. Biochem Biophys Res Commun 429: 148-155, 2012.
13. Gomes IM, Maia CJ and Santos CR: STEAP proteins: From structure to applications in cancer therapy. Mol Cancer Res 10: 573-587, 2012.
14. Oosterheert W and Gros P: Cryo-electron microscopy structure and potential enzymatic function of human six-transmembrane epithelial antigen of the prostate 1 (STEAP1). J Biol Chem 295: 9502-9512, 2020.
15. Nakamura H, Takada K, Arihara Y, Hayasaka N, Murase K, Iyama S, Kobune M, Miyanishi K and Kato J: Six-transmembrane epithelial antigen of the prostate 1 protects against increased oxidative stress via a nuclear erythroid 2-related factor pathway in colorectal cancer. Cancer Gene Ther 26: 313-322, 2019.
16. Menyhárt O, Nagy Á and Győrffy B: Determining consistent prognostic biomarkers of overall survival and vascular invasion in hepatocellular carcinoma. R Soc Open Sci 5: 181006, 2018.
17. Kanda Y: Investigation of the freely available easy-to-use software 'EZR' for medical statistics. Bone Marrow Transplant 48: 452-458, 2013.
18. Mani M, Carrasco DE, Zhang Y, Takada K, Gatt ME, Dutta-Simmons J, Ikeda H, Diaz-Griffero F, Pena-Cruz V, Bertagnolli M, *et al*: BCL9 promotes tumor progression by conferring enhanced proliferative, metastatic, and angiogenic properties to cancer cells. Cancer Res 69: 7577-7586, 2009.
19. Takada K, Zhu D, Bird GH, Sukhdeo K, Zhao JJ, Mani M, Lemieux M, Carrasco DE, Ryan J, Horst D, *et al*: Targeted disruption of the BCL9/β-catenin complex inhibits oncogenic Wnt signaling. Sci Transl Med 4: 148ra117, 2012.
20. Hayasaka N, Takada K, Nakamura H, Arihara Y, Kawano Y, Osuga T, Murase K, Kikuchi S, Iyama S, Emori M, *et al*: Combination of eribulin plus AKT inhibitor evokes synergistic cytotoxicity in soft tissue sarcoma cells. Sci Rep 9: 5759, 2019.
21. Matsuoka K, Koreth J, Kim HT, Bascug G, McDonough S, Kawano Y, Murase K, Cutler C, Ho VT, Alyea EP, *et al*: Low-dose interleukin-2 therapy restores regulatory T cell homeostasis in patients with chronic graft-versus-host disease. Sci Transl Med 5: 179ra43, 2013.
22. Llovet JM, Montal R, Sia D and Finn RS: Molecular therapies and precision medicine for hepatocellular carcinoma. Nat Rev Clin Oncol 15: 599-616, 2018.
23. Danila DC, Szmulewitz RZ, Vaishampayan U, Higano CS, Baron AD, Gilbert HN, Brunstein F, Milojic-Blair M, Wang B, Kabbarah O, *et al*: Phase I study of DSTP3086S, an antibody-drug conjugate targeting six-transmembrane epithelial antigen of prostate 1, in metastatic castration-resistant prostate cancer. J Clin Oncol 37: 3518-3527, 2019.
24. Dolezal JM, Wang H, Kulkarni S, Jackson L, Lu J, Ranganathan S, Goetzman ES, Bharathi SS, Beezhold K, Byersdorfer CA, *et al*: Sequential adaptive changes in a c-Myc-driven model of hepatocellular carcinoma. J Biol Chem 292: 10068-10086, 2017.
25. Zheng K, Cubero FJ and Nevzorova YA: c-MYC-making liver sick: Role of c-MYC in hepatic cell function, homeostasis and disease. Genes (Basel) 8: 123, 2017.
26. Grunewald TG, Diebold I, Esposito I, Plehm S, Hauer K, Thiel U, da Silva-Buttkus P, Neff F, Unland R, Müller-Tidow C, *et al*: STEAP1 is associated with the invasive and oxidative stress phenotype of Ewing tumors. Mol Cancer Res 10: 52-65, 2012.

Figure S1. Knockdown of *STEAP1* does not induce apoptosis in liver cancer cell lines. (A) HepG2 and (B) Hep3B cells were transfected with non-targeting control siRNA or siSTEAP1. Apoptosis was measured by flow cytometry using Annexin V/7-AAD staining. Data are presented as the mean of triplicate measurements ± SD. siRNA, small interfering RNA; STEAP1, six-transmembrane epithelial antigen of the prostate 1; N.S., not significant.

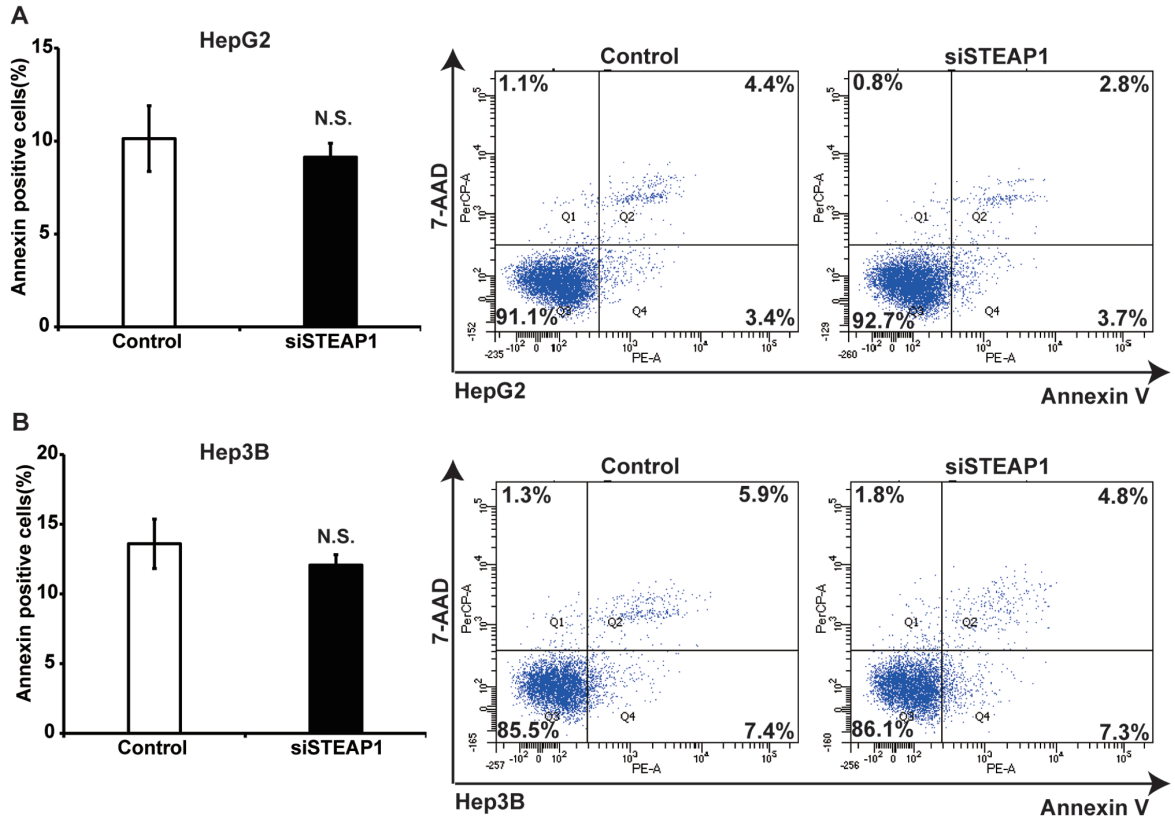

Figure S2. Pathways associated with high *STEAP1* expression were derived from GSEA. GSEA was performed to explore the gene sets regulated by *STEAP1* in hepatocellular carcinoma using the publicly accessible gene expression profiling dataset, GSE14520-GPL3921. Four statistically significant pathways, namely (A) MTORC1_SIGNALING, (B) MYC_TARGETS_V1, (C) UNFOLDED_PROTEIN_RESPONSE and (D) REACTIVE_OXYGEN_SPECIES_PATHWAY, are represented as enrichment plots. NOM P-val, nominal P-value; FDR Q-val, false discovery rate Q-value; GSEA, Gene Set Enrichment Analysis; NES, normalized enrichment score; STEAP1, six-transmembrane epithelial antigen of the prostate 1.

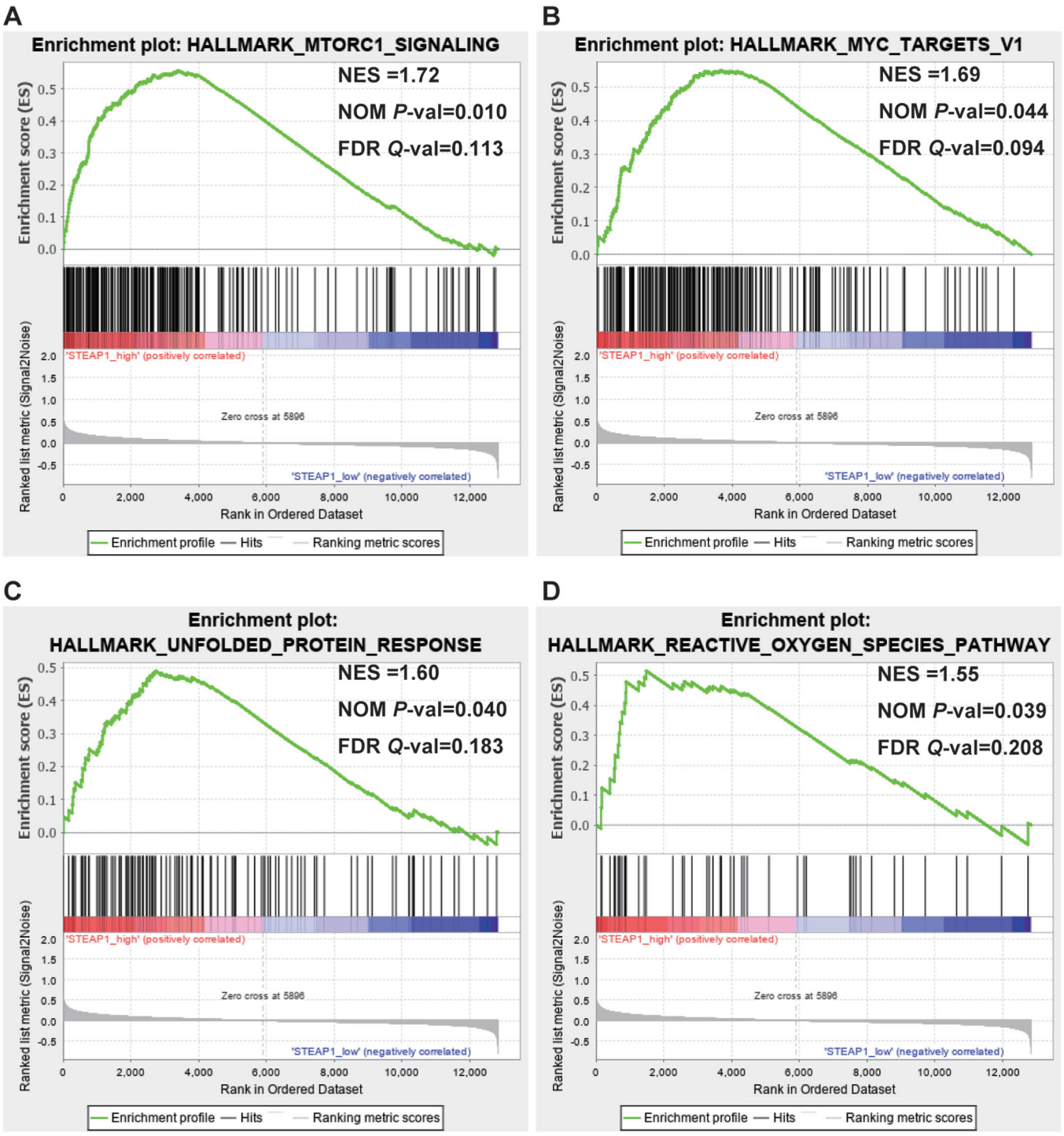

Figure S3. Inhibition of *STEAP1* suppresses c-Myc downstream target genes in HepG2 cells. HepG2 cells were transfected with non-targeting control siRNA and siSTEAP1. c-Myc downstream target genes were evaluated using PCR array. The 84 genes are listed in a (A) chart and (B) heatmap. Blue/purple represents a decreased expression level, and yellow represents no change. The numbers are indicating fold changes. siRNA, small interfering RNA; STEAP1, six-transmembrane epithelial antigen of the prostate 1.

A

Layout	01	02	03	04	05	06	07	08	09	10	11	12
A	AIMP2 -3.18	APEX1 -3.36	ATF4 -4.12	BAX -1.7	BCAT1 -1.55	CAD -6.13	CBX3 -1.54	CCNB1 -3.43	CCND2 -1.36	CCT5 -1.41	CDC25A -4.25	CDK4 -5.41
B	CDKN1B -3.74	CDKN2B -1.44	CHEK1 -3.54	CKS2 -1.93	YBX3 -1.92	CSDE1 -2.46	CSTB 1.2	CTSC -3.71	DDX10 -1.14	DDX39B -3.19	DKC1 -2.86	E2F1 -4.08
C	EIF4A1 -2.02	EIF4B -4.5	EIF4E -1.29	ENO1 -8.4	EXOSC8 -1.91	FASN -1.55	GCLC -1.54	GNL3 -2.04	HK2 -5.2	HNRNPA1 -1.87	HNRNPA2B1 -2.42	ID3 -8.45
D	ILK -2.2	ITGB1 -2.14	LTA4H -1.42	MAT2A -4.64	MAX -2.13	MAZ -1.94	MGST1 -1.27	MSH2 -1.86	MTHFD1 -5.94	MYC -2.16	MYCL -1.24	MYCN -5.44
E	NAP1L1 -3.02	NBN -1.08	NCL -3.16	NME1 -1.72	NOLC1 -5.82	NPM1 -2.35	ODC1 -2.83	PA2G4 -1.44	PAICS -3.32	PCNA -2.34	PDK1 -2.99	PHB -2.35
F	PIAS2 -2.43	POLD2 -2.34	PPAT -2.45	PPP2R4 -3.14	PSMG1 -1.7	PTEN 1.31	PYCR1 -3.91	RPL13 -1.27	RPL19 -1.04	RPL23 -1.44	RPL27A -1.15	RPL5 -2.27
G	RPS5 -4.55	SHMT1 -5.68	SNRPB -5.67	SRM -4.96	SRSF1 -3.23	TERT -2.14	TOP1 -3.44	TP53 -2.64	TPI1 -14.16	TYMS -1.82	UBE2C -2.17	ZFP36L1 1.2

B

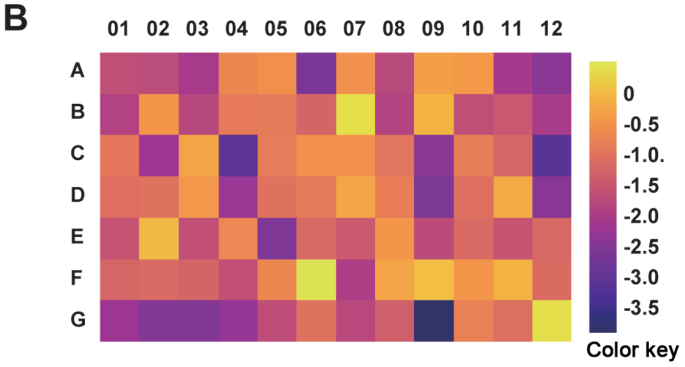

Figure S4. ROS production is increased by *STEAP1*-knockdown, but no statistical correlation between *STEAP1* and *NRF2* expression was observed in HCC. (A) HepG2 and (B) Hep3B cells were transfected with non-targeting control siRNA or si*STEAP1*. Cytosolic ROS levels were evaluated by flow cytometry using CellROX Deep Red. Data are presented as the mean of triplicate measurements ± SD. *P<0.05 vs. control. Correlation between *STEAP1* and *NRF2* expression in HCC samples using the publicly accessible gene expression profiling datasets, (C) GSE14520 and (D) GSE36376, and (E) TCGA. ROS, reactive oxygen species; NRF2, NF-E2-related factor 2; HCC, hepatocellular carcinoma; TCGA, The Cancer Genome Atlas; siRNA, small interfering RNA; STEAP1, six-transmembrane epithelial antigen of the prostate 1.

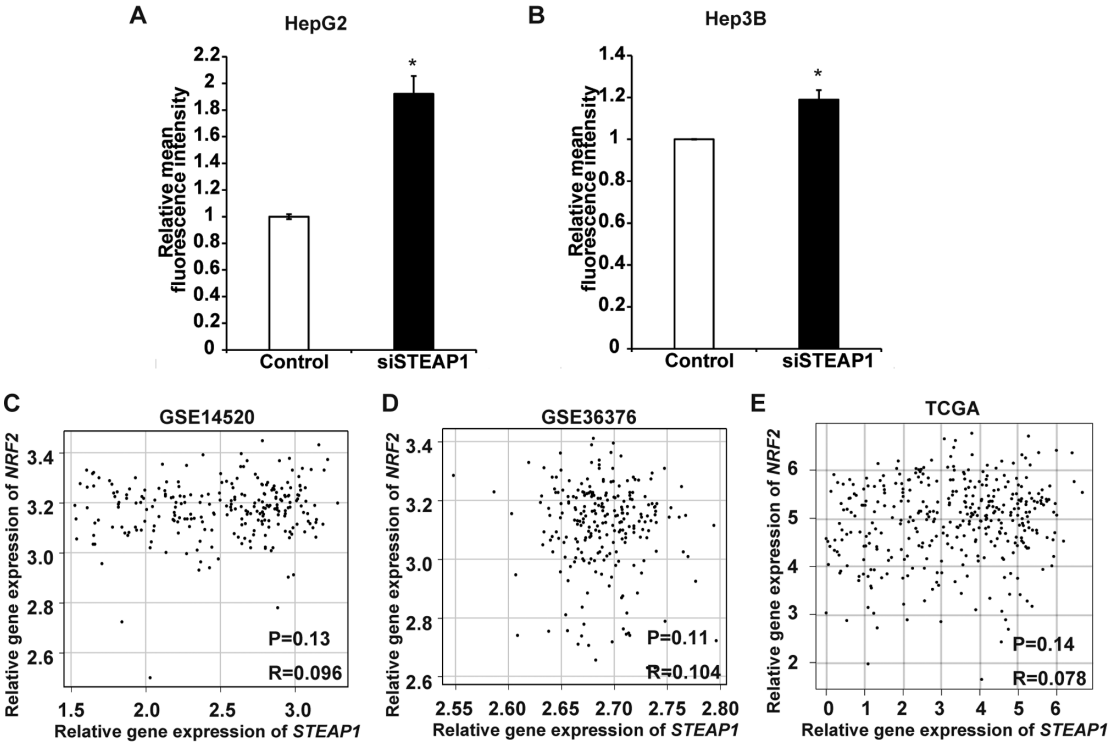

Table SI. List of enriched gene sets derived from Gene Set Enrichment Analysis in STEAP1-upregulated liver cancer using the publicly accessible gene expression profiling dataset, GSE14520-GPL3921.

Gene set	Size, bp	ES	NES	NOM P-value	FDR q-value	FWER P-value	Rank at max	Leading edge
HALLMARK_MYC_TARGETS_V2	58	0.69207776	1.8522855	0.004056795	0.037062958	0.025	2609	tags=67%, list=20%, signal=84%
HALLMARK_MTORC1_SIGNALING	198	0.55517286	1.7184767	0.009708738	0.112650275	0.13	3399	tags=64%, list=26%, signal=86%
HALLMARK_MYC_TARGETS_V1	199	0.5485847	1.691135	0.044265594	0.09423097	0.157	3651	tags=57%, list=28%, signal=79%
HALLMARK_UNFOLDED_PROTEIN_RESPONSE	111	0.49010047	1.5956153	0.03968254	0.18295158	0.301	2734	tags=46%, list=21%, signal=58%
HALLMARK_REACTIVE_OXYGEN_SPECIES_PATHWAY	46	0.51548195	1.5508558	0.0390625	0.20838094	0.367	1485	tags=33%, list=12%, signal=37%
HALLMARK_SPERMATOGENESIS	125	0.39619297	1.4034897	0.06036217	0.45093307	0.66	2142	tags=23%, list=17%, signal=28%
HALLMARK_UV_RESPONSE_UP	158	0.39965212	1.4012077	0.025096525	0.39195782	0.667	2467	tags=34%, list=19%, signal=42%
HALLMARK_IL6_JAK_STAT3_SIGNALING	87	0.48076102	1.3984529	0.115530305	0.3493785	0.673	2083	tags=34%, list=16%, signal=41%
HALLMARK_PI3K_AKT_MTOR_SIGNALING	102	0.35231537	1.3757539	0.06994329	0.35343066	0.717	2677	tags=36%, list=21%, signal=45%
HALLMARK_GLYCOLYSIS	188	0.39369822	1.3516054	0.04518664	0.36649844	0.763	1741	tags=29%, list=14%, signal=33%
HALLMARK_G2M_CHECKPOINT	198	0.5125287	1.3197974	0.22132796	0.3985368	0.817	2961	tags=48%, list=23%, signal=62%
HALLMARK_COMPLEMENT	188	0.37945133	1.2343261	0.19165085	0.5467972	0.904	3021	tags=36%, list=24%, signal=46%
HALLMARK_ALLOGRAFT_REJECTION	199	0.45003456	1.2291461	0.2626459	0.518129	0.912	2160	tags=33%, list=17%, signal=39%
HALLMARK_INFLAMMATORY_RESPONSE	192	0.4123962	1.2164818	0.22535211	0.5071917	0.921	2541	tags=32%, list=20%, signal=40%
HALLMARK_E2F_TARGETS	190	0.50353825	1.2131625	0.32416502	0.4807731	0.924	3011	tags=51%, list=23%, signal=66%
HALLMARK_IL2_STAT5_SIGNALING	176	0.37062678	1.2019329	0.15019011	0.4733342	0.933	1902	tags=32%, list=15%, signal=37%
HALLMARK_PROTEIN_SECRETION	96	0.35899216	1.1633826	0.28070176	0.52060544	0.954	2855	tags=36%, list=22%, signal=47%
HALLMARK_APICAL_SURFACE	34	0.36205694	1.120722	0.2993763	0.58005255	0.976	1708	tags=24%, list=13%, signal=27%
HALLMARK_CHOLESTEROL_HOMEOSTASIS	62	0.42461875	1.1076323	0.34179688	0.575295	0.98	2927	tags=45%, list=23%, signal=58%
HALLMARK_OXIDATIVE_PHOSPHORYLATION	200	0.34020543	1.0903395	0.42114696	0.58114666	0.984	3621	tags=39%, list=28%, signal=53%
HALLMARK_DNA_REPAIR	139	0.31362012	1.0856876	0.35510203	0.56315047	0.984	3269	tags=39%, list=25%, signal=52%
HALLMARK_TNFA_SIGNALING_VIA_NFKB	198	0.3788036	1.0426354	0.4123314	0.6192131	0.988	1380	tags=23%, list=11%, signal=25%
HALLMARK_HEME_METABOLISM	200	0.26369643	1.0405926	0.38649157	0.596399	0.988	2546	tags=25%, list=20%, signal=30%
HALLMARK_ANDROGEN_RESPONSE	100	0.29549375	1.0267878	0.4173077	0.59721136	0.99	2345	tags=27%, list=18%, signal=33%
HALLMARK_FATTY_ACID_METABOLISM	146	0.36947468	1.0193533	0.45724908	0.5859001	0.992	2310	tags=32%, list=18%, signal=38%
HALLMARK_ADIPOGENESIS	180	0.3029539	1.0026596	0.47134936	0.59420824	0.994	2268	tags=24%, list=18%, signal=29%
HALLMARK_ESTROGEN_RESPONSE_LATE	199	0.2794801	0.9988759	0.43796992	0.5792375	0.994	2004	tags=26%, list=16%, signal=30%
HALLMARK_MITOTIC_SPINDLE	178	0.3066864	0.9811845	0.4848485	0.5906945	0.996	1201	tags=17%, list=9%, signal=19%
HALLMARK_KRAS_SIGNALING_UP	196	0.29806554	0.9515187	0.54615384	0.6171569	0.997	2173	tags=27%, list=17%, signal=31%
HALLMARK_INTERFERON_GAMMA_RESPONSE	182	0.3532676	0.9378794	0.5162524	0.6206802	0.997	2377	tags=30%, list=19%, signal=37%
HALLMARK_HYPOXIA	195	0.29013985	0.9182161	0.5803922	0.63247	0.997	1593	tags=21%, list=12%, signal=23%
HALLMARK_APOPTOSIS	159	0.26394483	0.8810248	0.6206226	0.6772358	0.999	2364	tags=26%, list=18%, signal=31%
HALLMARK_INTERFERON_ALPHA_RESPONSE	83	0.3361705	0.8581146	0.62830186	0.69522154	1	2709	tags=34%, list=21%, signal=42%
HALLMARK_P53_PATHWAY	198	0.23427106	0.8421303	0.7685009	0.6997487	1	1911	tags=20%, list=15%, signal=23%
HALLMARK_PEROXISOME	99	0.23860918	0.705571	0.8519924	0.87374604	1	2721	tags=29%, list=21%, signal=37%
HALLMARK_COAGULATION	137	0.2352326	0.688134	0.905838	0.86841744	1	1613	tags=18%, list=13%, signal=20%

STEAP1, six-transmembrane epithelial antigen of the prostate 1; ES, enrichment score; NES, normalized ES; NOM, nominal; FDR, false discovery rate; FWER, family-wise error rate.